CHAPTER 5 FORMABILITY PREDICTION USING FORMING LIMIT DIAGRAM

From the previous chapter, it was found that different yield functions and hardening models led to dissimilar local stress and strain distributions for all investigated states of stress.

Thus, prediction of the failure onset could be definitely affected, in which a macrocrack in AHS steel sheets could occur before localized necking due to early damage initiation. This is challenging for the formability description. In general, the conventional forming limit diagram (FLD) is a well accepted tool for predicting formability behaviour of material in sheet metal forming processes. Nevertheless, in industrial applications, complex workpieces are usually manufactured in multi–step processes, whereby influences of the non–proportional strain history on the FLD could be problematic [1,88]. As shown, the forming limit stress diagram (FLSD) is less dependent on the forming history and strain path. It can be used to describe necking occurrences for any kind of drawn parts undergoing complex strain paths.

In this chapter, present an extensive effort for formability prediction of AHS steels with conventional FLDs, and demonstrate the FLSDs to characracterize the unique properties of theses steels. Additionally, this work have been precisely published in [41].The experimental and numerical analyses of Forming Limit Diagram (FLD) and Forming Limit Stress Diagram (FLSD) for two Advanced High Strength Steel (AHSS) sheets grade DP780 and TRIP780 were performed. Initially, the forming limit curves were experimentally determined by means of the Nakazima forming test. Subsequently, analytical calculations of both FLD and FLSD were carried out based on the Marciniack - Kuczinsky (M-K) model. Additionally, the FLSDs were calculated using the experimental FLD data for both investigated steels. Different yield criteria, namely, von Mises, Hill's 48, and Barlat2000 (Yld2000-2d) were applied for describing plastic flow behavior of the AHS steels. Both Swift and modified Voce strain hardening laws were taken into account. Hereby, influences of the constitutive yield models on the numerically determined FLDs and FLSDs were studied regarding to those resulted from the experimental data. The obtained stress based forming limits were significantly affected by the yield criterion and hardening model. It was found that the forming limit curves calculated by the combination of the Yld2000-2d yield criterion and Swift hardening law were in better agreement with the experimental curves. Finally, hole expansion tests were conducted in order to verify the different failure criteria. It was shown that the stress based forming limit curves could more precisely describe the formability behavior of both high strength steel sheets than the strain based forming limit curves.

5.1 INTRODUCTION

In the automotive industries, vehicles designed under consideration of light weight, crash performance, energy saving, and environmental aspect are of special interest. Using steel sheets with reduced thicknesses is desired as they lead to lower fuel consumption. However, at the same time passenger safety must be achieved by applying steels with increased ability of energy absorption. Thus, steel grades presenting both high strength and great formability are needed. To come to these requirements Advanced High Strength Steel (AHSS) grades such as Dual Phase (DP) steel,

Transformation Induced Plasticity (TRIP) steel and Complex (CP) steel have been continuously developed and employed [56,41,88]. In spite of their major advantage with respect to high strength to density ratio, low formability is a primary drawback of the AHS steels. A precise prediction of the forming limit has been hence extremely important for such novel steel grades. The concept of Forming Limit Diagram (FLD) was introduced by Keeler and Backofen and Goodwin [27,28]. Keeler et al. determined strains on the right hand side of the FLD and Goodwin extended the FLD by including negative minor strains. Further experimental investigations of the FLD were conducted for example by Ahmadi et al. [89].

Many researchers carried out experimental and theoretical analyses, which mostly showed that the maximum admissible limiting strains strongly depend on several physical factors, among which the most important ones are materials work-hardening, strain rate sensitivity, development of deformation mode or loading history, and plastic anisotropy induced by cold rolling process. It has been established that the FLD is sensitive to the pre-formed conditions of steel sheets, in particular non-linear deformation paths in a forming process. By industrial applications, complex work pieces are usually manufactured in multi-step processes. Thus, influence of the non-proportional strain history on the FLD can be critical. Under such conditions, the FLD cannot be applied to predict whether the forming process will be successful or failed [90]. In addition, several authors have proved that the FLD is only applicable for deformation with linear strain ratio [91,92]. Later, Arrieux [92] proposed a stress based forming limit concept, which seemed to be independent of the strain path changes. It was promoted as a solution for formability analysis in multi-stage forming processes. In a recent study, Stoughton [37] showed that an application of the stress based forming limit extended the validity of failure criterion for forming processes involving non-proportional loading.

By theoretical analysis for calculating limit strains and constructing FLDs of sheet metals, different materials models were investigated. Principally, for example, Swift [8] based model was proposed for describing diffuse necking and Hill [25] based model for localized necking. The model developed by Marciniak and Kuczinsky (M-K criterion) [15,26] is based on a thickness imperfection approach. This model has been one of the most widely applied models for FLD prediction.The failure strain depends mainly on the growth of an initial inhomogeneity presenting as a narrow band in material. Generally, accuracy of the predicted FLD can be significantly influenced by the shape of employed yield surface, hardening rule and strain rate sensitivity. For steel sheet materials, various yield functions and different hardening laws have been considered in the M-K criterion. The quadratic Hill's 48 yield criterion [6] has been successfully applied for steel sheets over a long period and is still widely used. Barlat and co-workers developed another series of yield functions, which was primarily focused on the description of plastic deformation of aluminum alloy. The first two models, Yld89 [93] and Yld91 [94] were proposed for sheet and bulk forming, respectively. Karafillis and Boyce [95] introduced an isotropic plasticity equivalent (IPE) model, which was used by Barlat et al. in the subsequent models Yld94 [96], Yld96 [97] and Yld2000 [7]. Recently, the Yld2000-2d yield criterion was increasingly applied for AHS steel grades [68,74,84-85,98-99]. It was shown that the Yld2000-2d model could predict more precisely plastic deformation behavior of the AHS steels as well. A theoretical study on forming limit diagrams was performed by Butuc et al. [91], in which the M–K theory was taken into account. Influences of different yield functions like von Misses isotropic

yield function, quadratic and non-quadratic criterion from Hill (Hill's 48 and Hill's 79) and Yld96 yield function on the predicted limit strains were examined. Two hardening models, namely Swift and Voce models, for the AA6016-T4 alloy was studied. The FLD predicted using Swift model was always higher than the simulated FLD using Voce model. It was found that an increase of balanced biaxial yield stress of the material led to a decrease of the limit strains in biaxial stretching region. A successful correlation between experiments and calculations was observed when yield locus was described by the Yld96 criterion and hardening behavior was represented by Voce model. Butuc et al. [91] also determined stress based forming limits from experimental strain data using the method proposed by Stoughton [37]. A bake hardened steel and an AA6016-T4 aluminum alloy were examined. Different yield criteria, for example, the Yld96 yield function were coupled with different hardening models in order to exhibit their influences on the calculated stress-based forming limits. In addition, influences of work hardening coefficient and strain rate sensitivity on the theoretical FLSDs were also evaluated. Irrelevant effect of the work-hardening coefficient was noticed. The predicted stress based forming limits decreased when the strain rate sensitivity increased. It was reported that that a combination of the strain based and stress based failure criterion could be a promising approach for sheet metal forming under multi-stage operations, when appropriate constitutive yield function was applied. S. Ahmadi et al. [89] demonstrated a study on theoretical prediction of FLDs for an AA3003-O aluminum alloy. The classical M–K model was utilized for simulating necking phenomenon and calculating limit strains. The employed yield functions were the BBC2000, BBC2002, and BBC200 yield criteria proposed by Banabic and co-workers [15,26,89]. It was observed that results from Voce hardening model were more precise than those from the Swift hardening model.

The main goal of this work was to investigate experimentally determined and theoretically calculated FLDs and FLSDs of two AHS steels, DP780 and TRIP780 steel. The FLDs and FLSDs based on experimental data were compared with the FLDs and FLSDs based on the M-K model. The influences of different hardening laws and yield criteria on the shape alteration of the FLDs and FLSDs were studied. Here, the hardening laws according to Swift and Voce, and the von Mises, Hill's 48, and Yld2000-2d yield criteria were considered. Uniaxial tensile test, hydraulic bulge test and disk compression test were carried out for obtaining required material parameters for the constitutive models. Subsequently, hole expansion tests were performed and simulated for both steels. The developed strain and stress values from the critical areas of the samples were plotted in the respective FLD and FLSD. Finally, the forming limit predictions using the FLD and the FLSD were compared with experimental results and discussed.

5.2 Experimental and Theoretical Strain and Stress Based Forming Limit

5.2.1 Strain Based Forming Limit

The FLD is often used as a conventional tool for formability prediction in sheet metal forming processes. The FLD is a strain based failure criterion, in which the principal in-plane strains at failure are evaluated. For experimental determination of the FLD for steel DP780 and TRIP780, the Nakazima test [30] was carried out according to the international standard ISO 120004-2 [61] on a 600 kN Erichsen sheet metal testing machine. The experimental test for constructing the FLDs was given in a more detail in Chapter 3 section 3.3.1

5.2.2 Stress Based Forming Limit

The stress based forming limit curve is represented by the principal in-plane stress components of the formed sheet samples. It was reported that the stress based criterion or the FLSD is more robust against any changes of strain path occurring in a forming process [37,100]. Since stress values cannot be determined directly in the Nakazima experiments, calculation of plastic deformation is needed. Based on the experimental forming limit strains and plasticity theory coupled with a yield criterion, the forming limit stress curves are computed [7,101-102]. A more description of the proposed equations for calculating the stress values are presented in Chapter2 section 2.3.4.1.

5.2.3 Theoretical Calculation of the Forming Limit

In this work, calculation of plastic instability was performed using the M-K (Marciniak-Kuczinsky) theory [26]. The rigid plasticity approach, plane stress condition and isotropic work hardening of the investigated material were assumed. The concept of M-K based analysis was schematically illustrated in Figure 5.1. The model is based on the growth of an initial defect in the form of a narrow band inclined at an angle ψ_0 with respect to the principal axis. The initial value of the geometrical defect is characterized by the ratio of the thickness in the groove by the thickness in the homogeneous region. The theoretical calculation to develop forming limit strain by M-K model was precisely described in a more detail in Chapter 2 section 2.3.3.2.

The M-K initial geometrical imperfection value is basically considered as an adjustable parameter in order to achieve the best accuracy of predicted results, for example Paraianu et al. [103] purposed a constant M-K imperfection value of 0.9995. In this work, the initial imperfection parameter f_0 of 0.9995 was also defined for calculations with the M-K model.The *x*, *y* and *z* axis correspond to the rolling, transverse, and normal directions of the steel sheet, respectively, whereas indexes 1 and 2 represent the principal stress or strain directions in the homogeneous region. The axes longitudinal and transverse to the groove direction are represented by the *n* and *t* axes, respectively. This proposed two-zone material model was subjected to plastic deformation by applying a constant incremental stretch on the homogeneous area. The plastic flow occurred in both regions and the evolution of strain rate difference between two zones was subsequently monitored.

The computations of strain rates in the homogeneous and heterogeneous zone were considered independently. Their relationship was obtained through the M-K conditions incorporating force equilibrium and geometrical compatibility. Small increments of equivalent strain were imposed to the homogeneous region. According to the plasticity theory, states of stress and strain in the homogeneous zone were computed. In order to define the strain and stress values for the heterogeneous zone, the Newton-Raphson method was applied for solving a system of two polynomial functions obtained by the yield criterion and the deformation compatibility requirement in the longitudinal direction of the necking band [102]. When the necking criterion was reached, the calculation was terminated and corresponding strains and stresses accumulated in the homogeneous zone at that moment were taken into account as the limit strains and limit stresses. The analysis was repeated for different initial orientations of groove by the angles between 0 and 90 degrees. The limit points for the FLD and FLSD were then obtained after minimization of the curves of principal strains and principal stresses, respectively, versus ψ_0 [26,102].

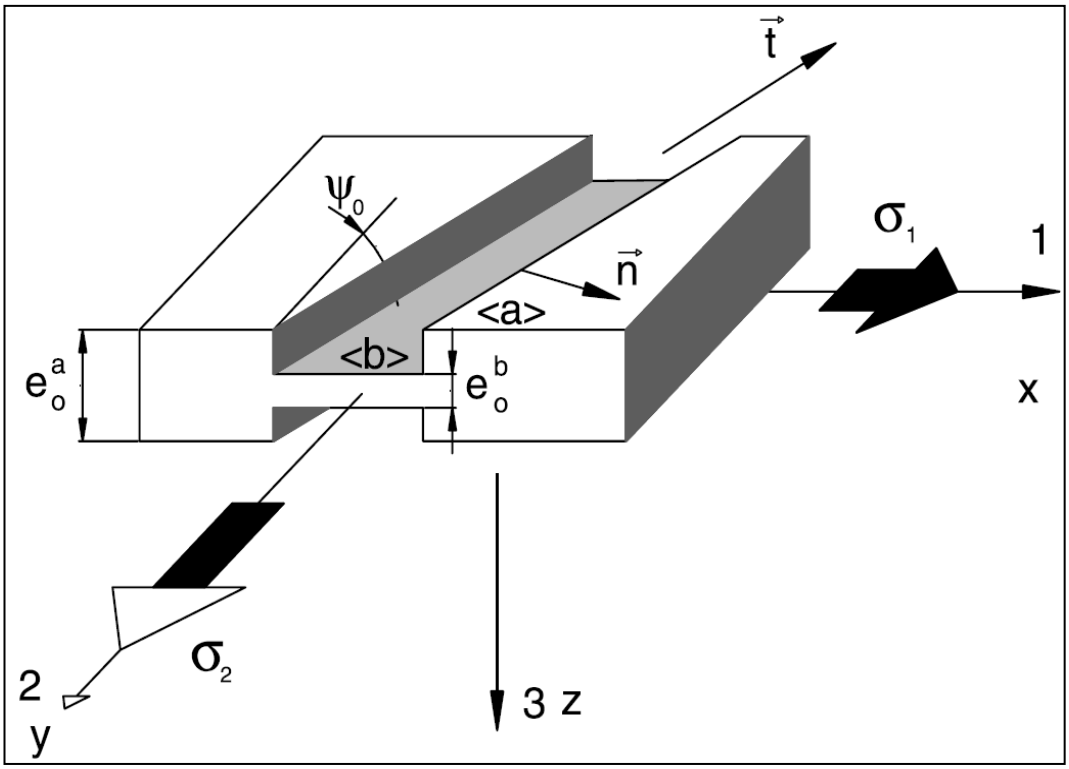

Figure 5.1 Geometric imperfection in the Marciniak – Kuczinsky model [26,101]

5.3 Materials Characterization

The commercial high strength steel sheets DP780 and TRIP780 with a thickness of 1.2 mm were investigated. The micrographs of both steels were illustrated in Figure 3.1(a) and Figure 3.1(b). The microstructure of the DP steel mainly consisted of martensitic islands embedded in a ferritic matrix. The microstructure of TRIP steel was that of a ferritic matrix containing bainite, retained austenite and small fraction of martensite. Phase transformation from the austenitic phase to martensite occurs when TRIP steel is subjected to a sufficient deformation. The formation of martensite increases the rate of work hardening, which, in turn, raises the ductility of the material. This typical TRIP effect causes the TRIP steel to generally exhibit higher elongation than the DP steel at a comparable tensile strength [56]. Note that the TRIP effect was not taken into account here, since the aim of this work was rather to study the effect of yield criteria on the predicted FLD and FLSD. However, its effect was fully accounted for in the determined stress-strain curve. Different mechanical tests were conducted in order to characterize the stress-strain behavior and to determine the material parameters for the applied hardening models. Simultaneously, the anisotropic coefficients were define by mechanical tests to obtain these parameters as expressed in a deeply explanation in section 3.1. Different yield criteria, namely, von Misses, Hill's 48 and Yld2000-2d in combination with the Swift hardening law and modified Voce hardening law were considered in the calculations of the FLD and FLSD for both investigated steels. A brief description of each model was summarized in section 2.2.

Furthermore, anisotropy coefficients of the anisotropic yield functions, Hill's 48 and Yld2000-2d, were calculated using the data from Tables 3.1 and 3.2. The coefficients for the Hill's 48 criterion obtained from the *r*-values at 0°, 45°, and 90° to the RD and the uniaxial yield stress in the RD were listed in Table 3.14 for both investigated steels.

For the Yld2000-2d criterion, the required parameters were the uniaxial yield stresses and the *r*-values from the directions 0°, 45° and 90° to the RD, the balanced biaxial flow stress and the balanced biaxial r_b value. These eight experimentally determined properties, namely, flow stresses $\sigma_0, \sigma_{45}, \sigma_{90}, \sigma_b$ and *r*-values r_0, r_{45}, r_{90}, r_b in conjunction with a system of non-linear algebraic equations were used to determine the coefficients α_i, i = 1….8 in [7]. Since the DP780 and TRIP780 steels mainly consisted of the ferritic structure, the m exponent of the Yld2000-2d model was set to be 6, which has been recommended for metals with BCC lattice. The anisotropy coefficients calculated from the yield stresses and *r*-values were summarized in Table 3.15 and 3.16 for the DP780 and TRIP780 steels, respectively. Additionally, stress-strain curves from bulge test for the DP780 and TRIP780 steels were fitted and extrapolated with the Swift and modified Voce hardening law. The resulted material parameters were listed in Table 3.17 and Table 3.18, respectively.

5.4 Results and Discussion

5.4.1 Forming Limit Diagrams

From the experimental Nakazima stretching tests with the strain optical measurement Autogrid system, the FLDs of the investigated steels, DP780 and TRIP780, were determined and shown in Figure. 5.2. The forming limit curve of the TRIP780 steel was slightly higher than that curve of the DP780 steel in both positive and negative minor strain regions. This was likely due to the higher strain hardening rate of the TRIP780 steel than that of the DP780 steel, as represented by the strain hardening exponent *n*, listed in Tables 3.17 and 3.18, or as illustrated in Figure 3.17 in form of stress-strain curves. The stress-strain curves obtained from uniaxial tensile tests in the RD and bulge tests were compared with the stress-strain curves extrapolated by the Swift and Voce laws for the investigated steels in Figure 3.17. It could be observed that higher strain hardening exponent led to an increase in the forming limit strains in all states of stress from uniaxial tension to biaxial deformation. The higher strain hardening caused a delay of necking during deformation process. The influences of the strain hardening law and yield criterion on the predicted FLDs were shown in Figure 5.4 and Figure 5.5 for the DP780 and TRIP780 steels, respectively. Figure 5.4 showed the experimentally and theoretically determined FLDs for the DP780 steel using different combinations of Swift and modified Voce hardening law with the von Mises, Hill's 48, and Yld2000-2d yield criterion. The M-K model was employed to calculate the critical strains for various states of stress, in which the initial imperfection parameter f_0 of 0.9995 was defined. Obviously, among all applied model combinations, the theoretical forming limit curve calculated by the Swift hardening model coupled with the Yld2000-2d yield function was in best agreement with the experimental curve, especially on the right hand side of the diagram. Nevertheless, on the left hand side, particularly in uniaxial tension, the predicted forming limit curves underestimated the experimental curve, to an extent that depended on the used constitutive models. In this region, critical strains calculated using the von Mises and Hill's 48 yield criteria slightly differed from those using the Yld2000-2d model for both Swift and modified Voce hardening laws. Here, the hardening laws exhibited larger effects than the yield criteria, in which the Swift model definitely provided higher limit strains than the modified Voce model. In the biaxial range on the right hand side, forming limit strains calculated by the von Mises and Hill's 48 models were significantly different from those calculated by the Yld2000-2d yield model and from the experimental data.

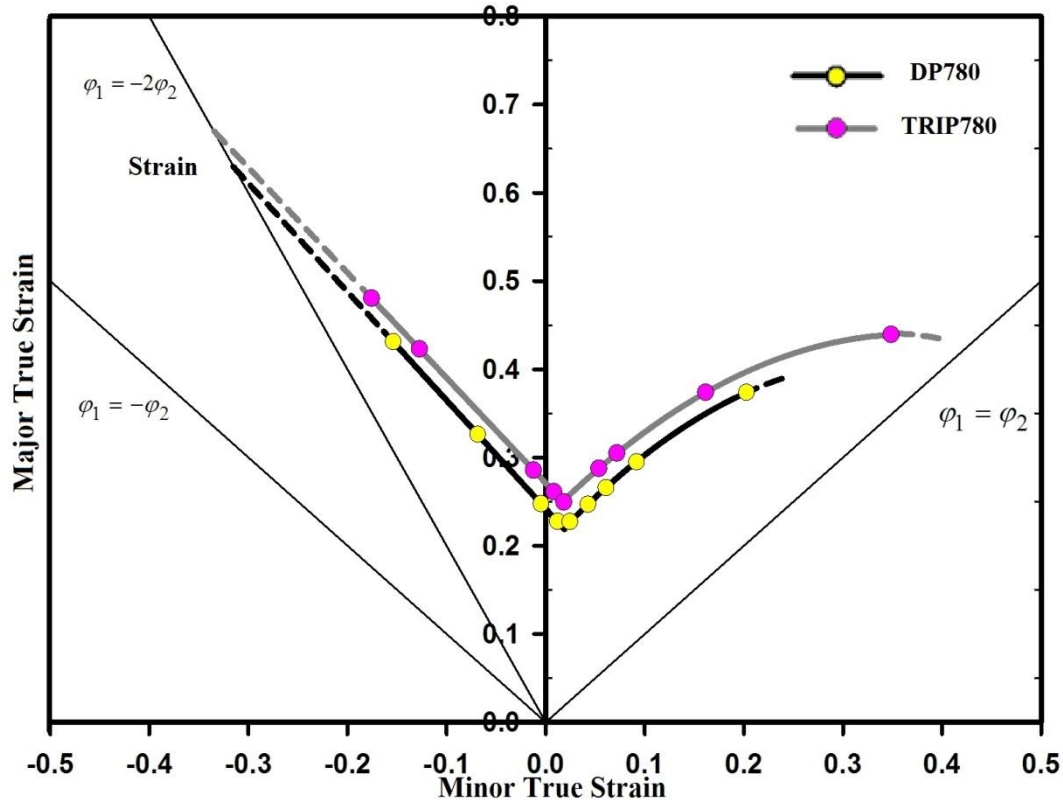

Figure 5.2 Experimentally determined FLDs of the investigated DP780 and TRIP780 Steels

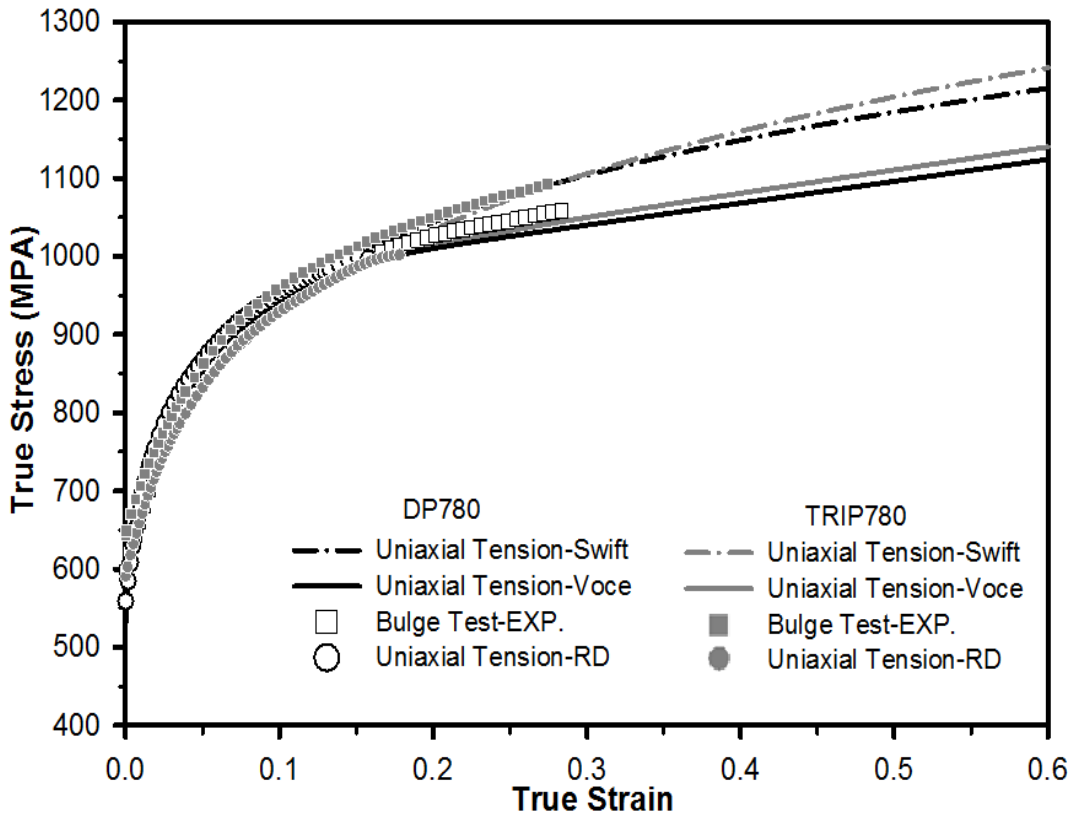

Figure 5.3 Experimental and extrapolated stress-strain curves of the investigated steels

The theoretical FLD of the DP780 steel based on the modified Voce hardening law were much lower than the experimental FLD in the uniaxial and plane strain state, but higher in the biaxial state. In contrast, the Swift law provided critical strains which were rather closer to the experimental results in the left hand region. It could be observed that the von Mises and Hill's 48 models gave acceptable limit strains on the left hand region when combined with the Swift hardening law, but not on the right hand region. The limit biaxial strains were considerably improved when coupled with the Yld2000-2d yield criterion. In plane-strain area, limit strains were more accurately predicted by the Swift law as same as in the uniaxial state. The experimentally determined and theoretically calculated FLDs of the TRIP780 steel were compared in Figure 5.5. Similar prediction trends and results as discussed for the DP780 steel were found. Thus, it could be concluded, that the theoretically determined forming limit curves of the DP780 and TRIP780 steel sheets based on the Swift hardening law in combination with the Yld2000-2d yield criterion led to the most precise results. In particular, from plane strain to balanced biaxial stretching regions, experimental and calculated FLDs were acceptable although, on the left hand side of the FLDs, predicted limit strains based on this model combination underestimated the experimental data. The predictions of the FLDs using other combined models were worse for both steels. The forming limit curves calculated by the M-K model were significantly affected by the yield criterion as well as hardening law.

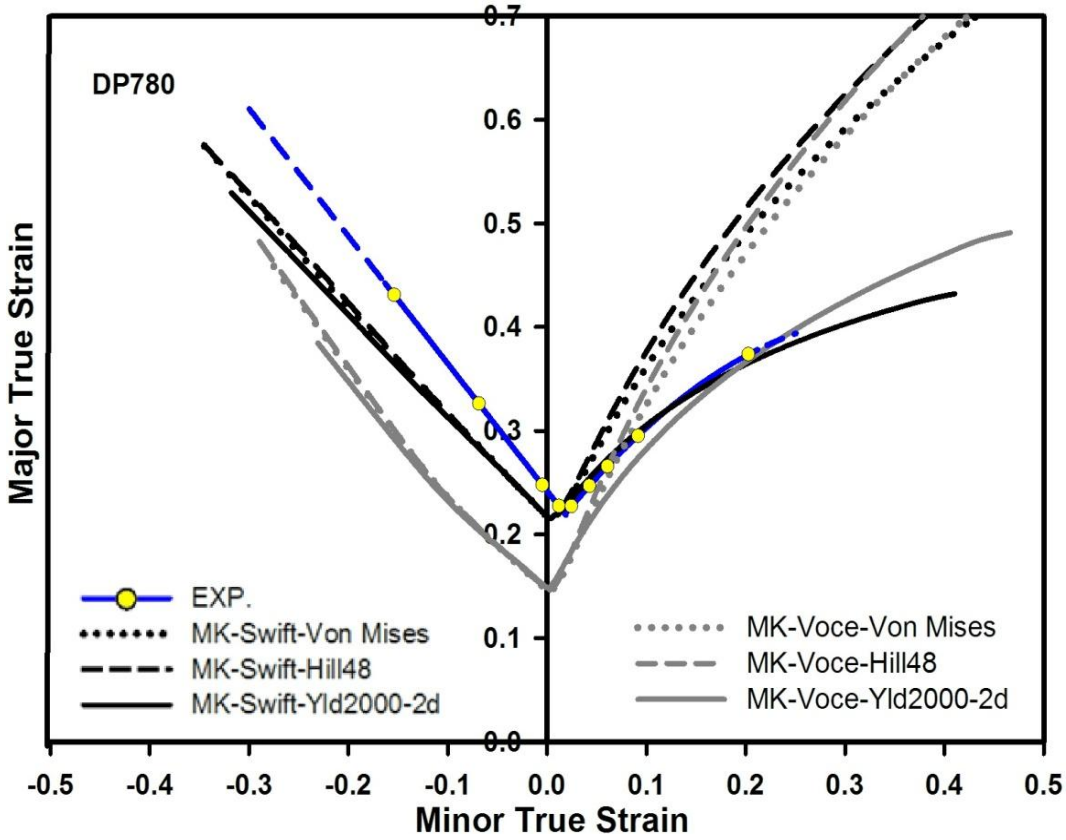

Figure 5.4 Comparison between experimentally determined and theoretically calculated FLDs for the DP780 steel

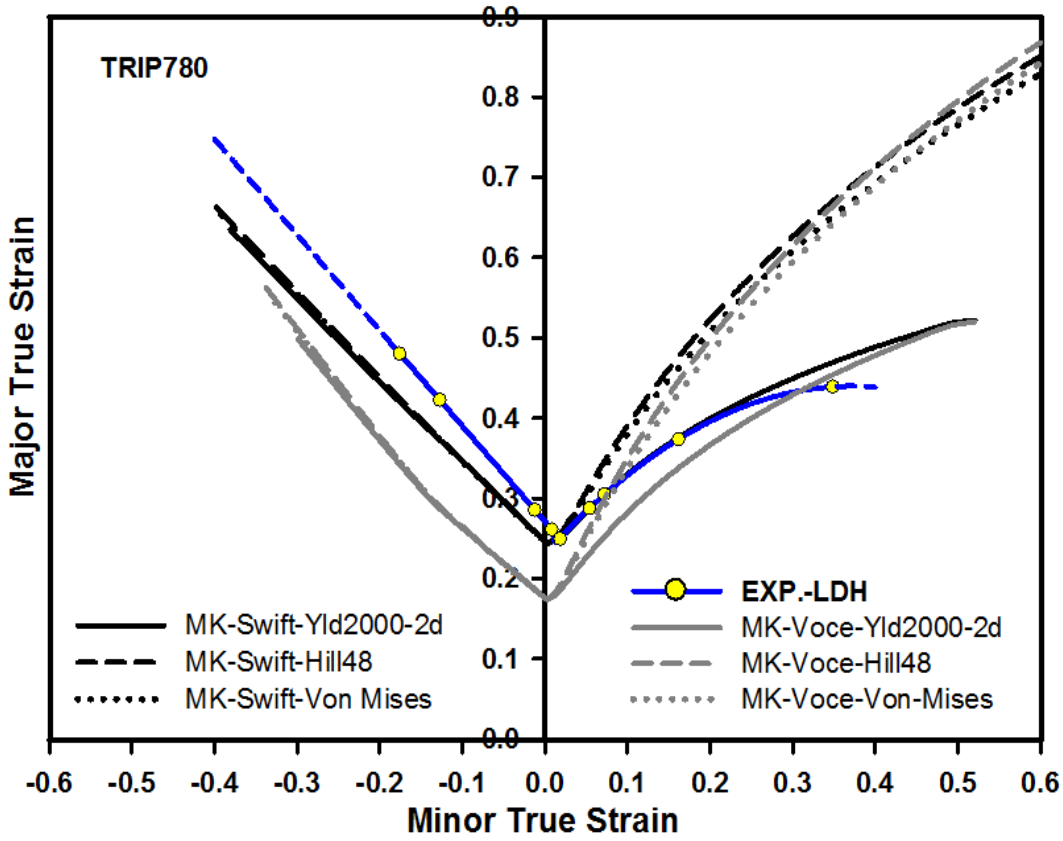

Figure 5.5 Comparison between experimentally determined and theoretically calculated FLDs for the TRIP780 steel

5.4.2 Forming Limit Stress Diagram

The calculation of plasticity was performed for determining the forming limit stress diagrams, as presented in section 5.2.2. The influences of various combinations of yield criterion and hardening law on the predicted critical stresses were studied. First, FLSDs of both DP780 and TRIP780 steels were calculated with regard to the experimental forming limit curve of the corresponding steels. In turn, the Swift and modified Voce hardening law in combination with the yield criterion according to the von Mises, Hill's 48 and Yld2000-2d models were taken into account for the calculation. Figure 5.6 showed the experimentally based FLSDs determined by different models in comparison. Generally, it could be found that the Swift hardening law provided higher forming limit stresses than the modified Voce hardening law whichever yield criterion was applied. The same yield criterion gave similar limit stress developing along all states of stress from the uniaxial to the biaxial regions. Obviously, the von Mises model exhibited higher critical limit stresses than the Hill's 48 and Yld2000-2d model. The FLSDs calculated by the Yld2000-2d model were more uniformly distributed than those calculated by other models, except near the area of balanced biaxial tension, where a little increase of limit stress was provided. Similar results were obtained for the TRIP780 steel and, therefore, were not depicted here.

Subsequently, FLSDs for both steels were determined based on the corresponding FLDs from the Nakazima stretching tests and predicted by the M-K model. By the same manner, influences of hardening law and yield criterion on the obtained FLSDs were investigated.

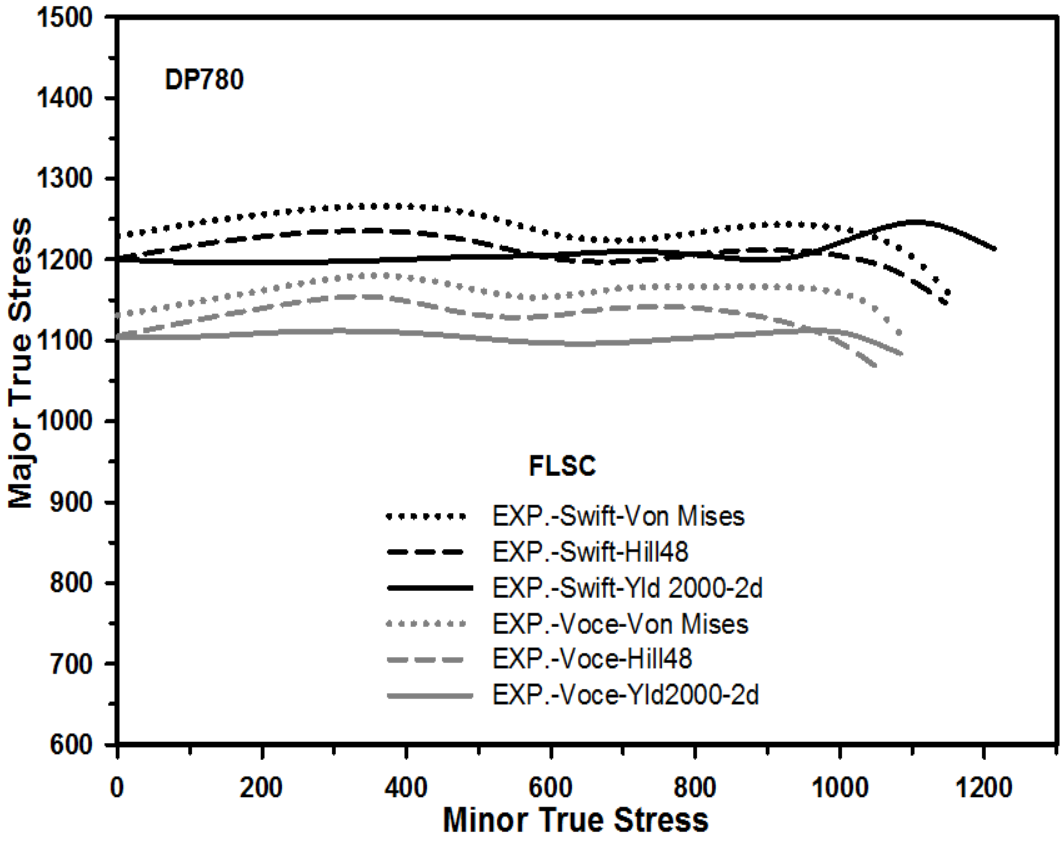

Figure 5.6 Determined FLSDs based on the experimental FLDs and different yield criteria and hardening models for the DP780 steel.

In Figure 5.7, the FLSDs calculated using the experimental data and M-K failure model were compared. The FLSD calculated from the M-K model fairly agreed with the FLSD based on the experimental FLD when the Swift hardening law was coupled with the Yld2000-2d yield criterion. However, in the uniaxial state of stress the forming limit stresses according to the FLD predicted by the M-K model slightly underestimated the critical stresses obtained from the experimental FLD. In contrast, in the biaxial state of stress limit stresses based on the M-K model a bit overestimated those calculated from the experimental FLD. This was due to the discrepancy between the experimentally and theoretically determined FLDs. By using other yield criteria deviations between forming limit stresses calculated by M-K model and experimental data became considerable.

For example, in case of the Swift hardening law coupled with the Hill's 48 model the FLSD with regard to the experimental FLD much differed from the FLSDs with regard to the FLD based on the M-K model for the whole state of stress. Additionally, it was observed that, by applying the modified Voce or Swift hardening model with Yld2000-2d yield criterion, the critical limit stresses based on the experimental FLD were a bit higher in the uniaxial stress state, and lower in the biaxial stress state than those based on the M-K model. It could be noticed that the M-K model in combination with the Swift hardening model and the Yld2000-2d yield criterion more precisely predicted the FLSD than other models. Similar results and trends were found for the TRIP780 steel.

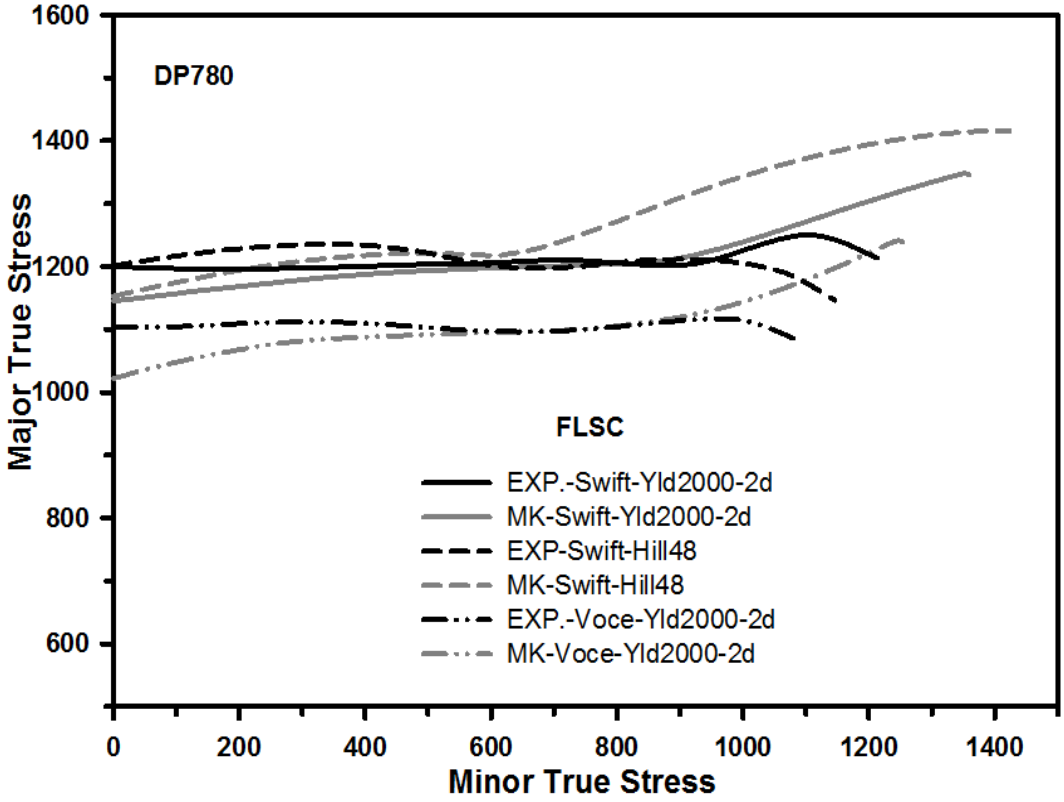

Figure 5.7 Comparison between determined FLSDs based on the FLDs obtained by experiments and M-K model for the DP780 steel

5.5 Application

As mentioned, in a complex or multi-step forming process, where the strain path is non-proportional, the FLD can be displaced depending on the forming history changes. To some extent, the FLSD has been proved to be more robust against such conditions. In order to demonstrate the application of the determined FLDs and FLSDs, hole expansion tests with flat bottom punch were conducted. In the experiments, sheet samples with a wire cut hole in the middle were drawn with a flat punch until the first crack appeared. Setup schematic of the hole expansion test was presented in Figure 5.8 [1]. In this study, an initial hole diameter of 12 mm was used. The hole expansion test provided a special procedure for evaluating stretch-flangeability of material, in which radial compressive and tangential tensile stresses were allowed simultaneously in the vicinity of the hole area [6]. Critical state of stress occurred in the hole expansion test located on the left hand side of the strain based diagram between uniaxial and plane strain tension. Subsequently, FE simulations of the hole expansion test with the same boundary conditions were carried out for both DP780 and TRIP780 steels. Note that no special failure criterion was defined in the FE simulations. The force-displacement curves from the experiments and FE simulations were determined and compared in order to verify the simulation results and to identify the point of time when failure took place during the experiments.

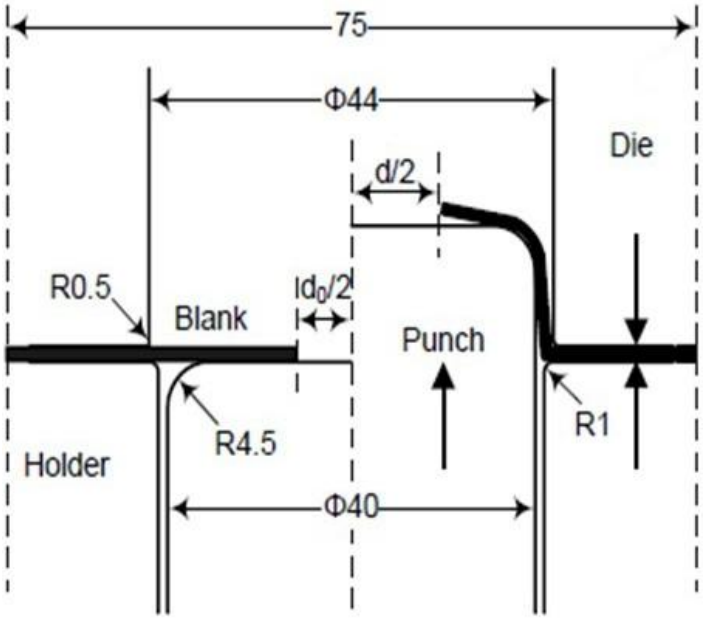

Figure 5.8 Schematic of hole expansion test with flat bottom punch [1]

The strain paths of crack initiating element up to the failure or maximum load in the hole expansion experiments calculated by the FE simulations were illustrated with the experimental FLDs for the DP780 and TRIP780 steels in Figure 5.9 and Figure 5.10, respectively. Different yield criteria were hereby taken into account. From these diagrams, it was obvious that deformed samples of both steels failed during hole expansion before the strains reached the predicted FLD. The strain paths until the experimental failure ended far below the forming limit strains. By this consideration it could be predicted that strain path continues in a linear manner and the material will not fail. Nevertheless, it was noticed that the state of strain at failure for both investigated steels could not be accurately described by the FLD. Therefore, predictions of crack initiation during forming, as presented in Figure 5.9 and Figure 5.10, were not satisfactory. The strain path resulted from different yield criteria exhibited small discrepancies in the values of the intermediate strains as well as the failure strains. For both investigated steels, the predicted strains at failure with respect to the Swift hardening model coupled with the Hill'48 yield function was closer to the experimental forming limit curves than those predicted with other yield criteria. The strain paths obtained from the von Mises and Yld2000-2d criteria were very similar to each other.

With respect to the results discussed above, the predictions based on the Swift hardening law coupled with the Yld2000-2d yield function were in better agreement with the experimental data for both investigated steels than those with other models. Thus, the FLSDs determined based on the experimental FLD, using the Yld2000-2d yield criterion and the Swift hardening law were considered for the verification. The forming limit stresses for the TRIP780 steel were higher than the critical stresses for the DP780 steel, as depicted in Figure 5.10, since the yield stress and strain hardening rate of TRIP780 were slightly higher than those of the DP780 steel.

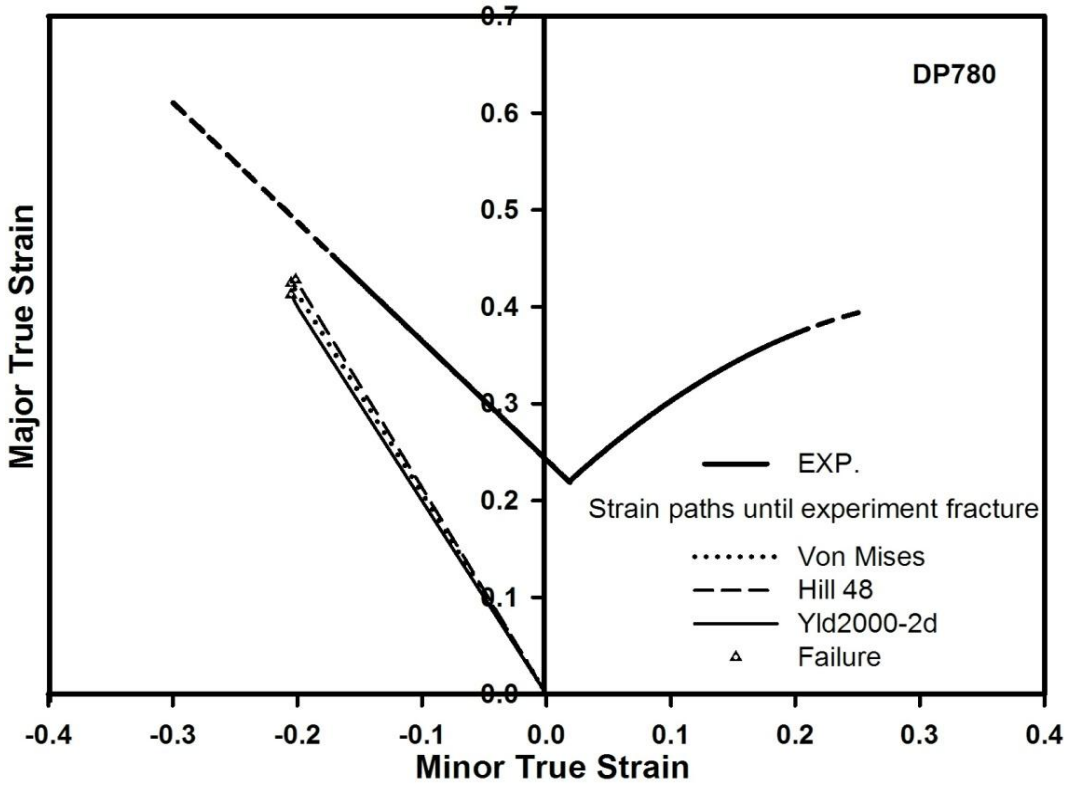

Figure 5.9 Strain paths from the hole expansion test until experimental failure calculated using different yield criteria and Swift hardening law in the FLD of the DP780 steel.

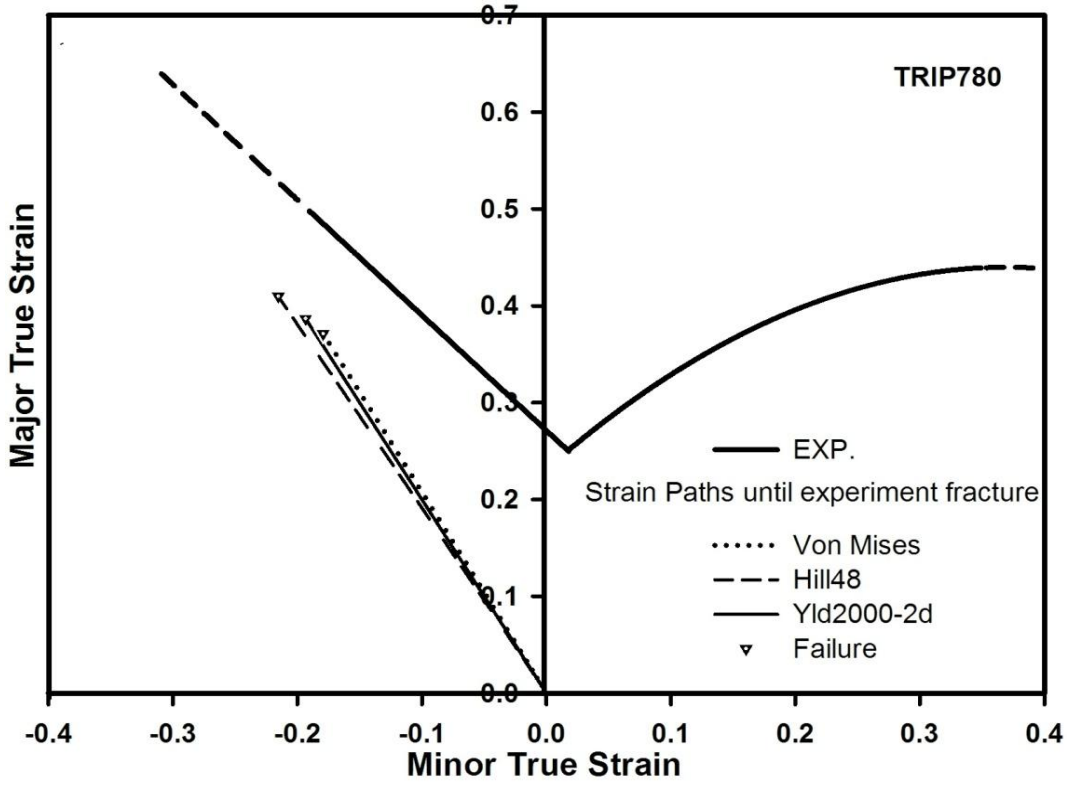

Figure 5.10 Strain paths from the hole expansion test until experimental failure calculated using different yield criteria and Swift hardening law in the FLD of the TRIP780

The FLSDs were plotted together with the calculated stress paths from the hole expansion test simulations up to the experimental point of fracture for both steels, as demonstrated in Figure 5.11. In this diagram, it was found that the critical stresses at failure from forming histories of the hole expansion tests were very close to the FLSD values based on the experimental FLD. The stress based forming limit, or the FLSD, better predicted the failure state of both investigated steels. Thus, the stress based failure criterion FLSD could reproduce local deformation conditions during cracking more realistically than the strain based failure criterion FLD. Hence, it was established that the strain based forming limit or the FLD was not applicable to the hole expansion test, the stress based forming limit diagram based on the experimental FLD rather led to more accurate failure predictions of high strength steels under such loading condition.

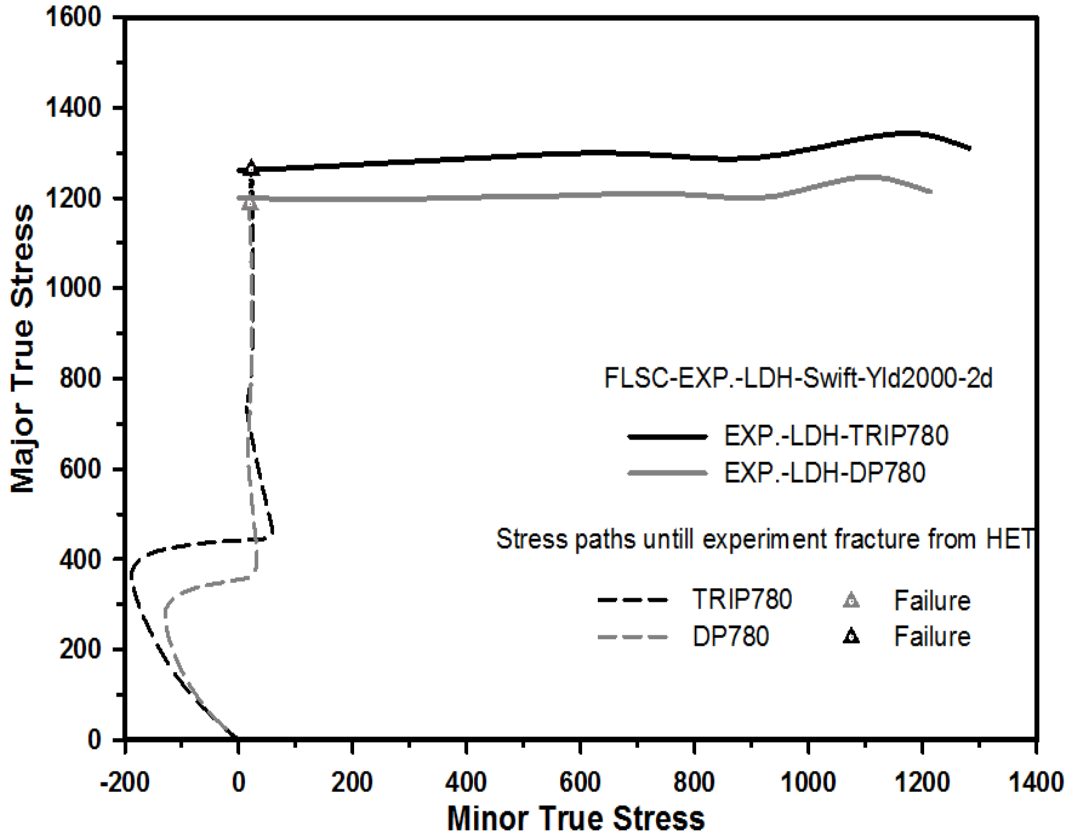

Figure 5.11 Stress paths from the hole expansion test until experimental failure calculated using Yld2000-2d yield criterion and Swift hardening law in the FLSD based on the experimental FLD data of the DP780 and TRIP780 steels

5.6 Conclusions

In this work, the FLD of high strength steel sheets DP780 and TRIP780 were experimentally determined by performing the Nakazima stretching test. Additionally, the theoretical FLDs and FLSDs based on the M-K model were calculated using the Swift and modified Voce hardening law coupled with different yield functions, von Mises, Hill's 48 and Yld2000-2d. The FLSDs were calculated based on the experimental FLD data as well. By comparison between the experimentally and

theoretically obtained FLDs for both investigated steels, it was concluded that the M-K model in combination with the Swift hardening law and the Yld2000-2d yield criterion provided the most accurate formability prediction, in particular from plane strain to balanced biaxial tension. Nevertheless, the experimental FLDs were slightly underestimated under the uniaxial tension load. Regarding the stress based criterion, calculated FLSDs were significantly affected by the applied yield criteria and hardening laws. The Swift hardening law provided higher forming limit stresses than the modified Voce model in entire states of stress. The yield function showed considerable effects on the shape of the FLSD. The FLSDs based on the FLD predicted by the M-K model in combination with the Swift hardening model and Yld2000-2d yield criterion better agreed with the FLSDs based on the experimental FLD than other models. However, small discrepancies of the limit stresses were observed in the uniaxial tension and biaxial stress states. According to the hole expansion test, it was verified that the conventional FLDs was insufficient for predicting material failure in sheet forming process, whereas the FLSDs could more precisely describe the formability limit of both high strength steels. The stress based failure criterion fairly represented local deformation at crack initiation than the strain based failure criterion. Indeed, accuracy of the FLSD depended strongly on the yield function and hardening law applied in the calculations.